

UCSF

UC San Francisco Previously Published Works

Title

Caspase-8 restricts antiviral CD8 T cell hyperaccumulation

Permalink

<https://escholarship.org/uc/item/8cj078p4>

Journal

Proceedings of the National Academy of Sciences of the United States of America, 116(30)

ISSN

0027-8424

Authors

Feng, Yanjun
Daley-Bauer, Lisa P
Roback, Linda
et al.

Publication Date

2019-07-23

DOI

10.1073/pnas.1904319116

Peer reviewed



Caspase-8 restricts antiviral CD8 T cell hyperaccumulation

YanJun Feng^a, Lisa P. Daley-Bauer^a, Linda Roback^a, Hongyan Guo^a, Heather S. Koehler^a, Marc Potempa^{b,c}, Lewis L. Lanier^{b,c,1}, and Edward S. Mocarski^{a,1}

^aDepartment of Microbiology and Immunology, Emory Vaccine Center, Emory University School of Medicine, Atlanta, GA 30033; ^bDepartment of Microbiology and Immunology, University of California, San Francisco, CA 94143; and ^cParker Institute for Cancer Immunotherapy, University of California, San Francisco, CA 94143

Contributed by Lewis L. Lanier, June 10, 2019 (sent for review March 14, 2019; reviewed by Mariapia Degli-Esposti and Jianke Zhang)

The magnitude of CD8 T cell responses against viruses is checked by the balance of proliferation and death. Caspase-8 (CASP8) has the potential to influence response characteristics through initiation of apoptosis, suppression of necroptosis, and modulation of cell death-independent signal transduction. Mice deficient in CASP8 and RIPK3 (*Casp8^{-/-}Ripk3^{-/-}*) mount enhanced peak CD8 T cell levels against the natural mouse pathogen murine cytomegalovirus (MCMV) or the human pathogen herpes simplex virus-1 compared with littermate control RIPK3-deficient or WT C57BL/6 mice, suggesting an impact of CASP8 on the magnitude of antiviral CD8 T cell expansion and not on contraction. The higher peak response to MCMV in *Casp8^{-/-}Ripk3^{-/-}* mice resulted from accumulation of greater numbers of terminally differentiated KLRG1^{hi} effector CD8 T cell subsets. Antiviral *Casp8^{-/-}Ripk3^{-/-}* T cells exhibited enhanced proliferation when splenocytes were transferred into WT recipient mice. Thus, cell-autonomous CASP8 normally restricts CD8 T cell proliferation following T cell receptor activation in response to foreign antigen. Memory inflation is a hallmark quality of the T cell response to cytomegalovirus infection. Surprisingly, MCMV-specific memory inflation was not sustained long-term in *Casp8^{-/-}Ripk3^{-/-}* mice even though these mice retained immunity to secondary challenge. In addition, the accumulation of abnormal B220⁺CD3⁺ T cells in these viable CASP8-deficient mice was reduced by chronic MCMV infection. Combined, these data bring to light the cell death-independent role of CASP8 during CD8 T cell expansion in mice lacking the confounding impact of RIPK3-mediated necroptosis.

apoptosis | necroptosis | cell death | ripoptosome | herpesvirus

In response to virus infection, naïve CD8 T cells expand dramatically and differentiate into heterogeneous subsets exhibiting differences in antigen specificity, memory potential, and effector function. Subsequently, most T cells contract as antigen levels decline, leaving a long-lasting memory pool that protects the host from reinfection (1, 2). During the acute phase of infection, a prominent, terminally differentiated and short-lived T cell subset expresses high levels of killer cell lectin-like receptor G1 (KLRG1) and low levels of IL-7R α (CD127). While KLRG1^{hi}CD127^{lo} terminal effector cells perform robust cytotoxic killing to bring viral infection under control, this subset is mostly eliminated through the contraction phase of the immune response (3). In contrast, the less terminally differentiated KLRG1^{lo}CD127^{hi} cells survive and contribute to immune memory. KLRG1^{hi}CD127^{hi} cells may down-regulate KLRG1 during contraction and also contribute to memory (4). Most of these features apply to conventional epitope-specific CD8 T cells responding to murine cytomegalovirus (MCMV), a natural mouse herpesvirus (5). MCMV induces conventional T cell responses that follow classic kinetics, with phases of expansion and contraction resulting in T cells with a central memory (T_{cm}) phenotype (CD62L^{hi}KLRG1^{lo}CD127^{hi}). MCMV also drives hallmark inflationary T cell responses (6) characterized by an effector T cell phenotype (CD62L^{lo}KLRG1^{hi}CD127^{lo}). These cells continue to expand during lifelong latency, giving rise to memory inflation that is dependent on sporadic antigen

production during episodes of viral reactivation (6, 7). This hallmark pattern is characteristic of human CMV- as well as MCMV-specific immunity (5). The magnitude and phenotype of inflationary and conventional T cell subsets are influenced by the antigen load, costimulatory molecule signaling, and cytokine milieu that together balance cell proliferation, death, and differentiation. On balance, acute infection is thereby controlled and lifelong latent infection is maintained (5).

T cell numbers are regulated through intrinsic (mitochondrial) as well as extrinsic cell death pathways (8). Intrinsic apoptosis, regulated by Bcl-2 family members, has long been known to control the elimination of CD8 T cells in the thymus, during postthymic homeostasis, and throughout the robust expansion and contraction phases governing the response to foreign antigen (3, 9, 10). Bcl-2 family member Bim is the major activator of the effector proteins Bax and Bak, directing their localization to mitochondria to eliminate antiviral T cells during contraction of the immune response (9, 10). Extrinsic death appears to restrict postthymic homeostasis and collaborate with intrinsic apoptosis during contraction (11). The TNF superfamily death receptor (DR), Fas (CD95), has long been known to mediate the formation of a death-inducing signaling complex (DISC), where Fas-associated death domain protein (FADD) recruits caspase (CASP)8 to drive CASP3-dependent cell death independently of Bim, Bak, and Bax (9, 10). The long form of FLIP (cFLIP_L),

Significance

The antiviral immune response in mammals represents a balance of T cell proliferation and death. The autoactivated protease caspase-8 has long been known to mediate cell-extrinsic apoptosis, block unleashed programmed necrosis, and contribute to cell activation state as well as cell growth. Here, caspase-8 is shown to restrict proliferation of CD8 T cells in response to herpesvirus infection without contributing to the contraction of the immune response. Prior investigations into this area were confounded by unleashed necroptosis, masking the role of caspase-8 in restraining proliferation associated with adaptive immunity. Thus, our observations resolve a decades-old debate regarding the cell-autonomous contribution of this protease to initiation of antiviral T cell immunity and establishment of memory.

Author contributions: Y.F., L.P.D.-B., H.S.K., L.L.L., and E.S.M. designed research; Y.F., L.P.D.-B., L.R., H.G., H.S.K., and M.P. performed research; H.G., H.S.K., M.P., and L.L.L. contributed new reagents/analytic tools; Y.F., L.P.D.-B., and L.L.L. analyzed data; and Y.F., L.P.D.-B., and E.S.M. wrote the paper.

Reviewers: M.D.-E., Monash University; and J.Z., Thomas Jefferson University.

The authors declare no conflict of interest.

Published under the PNAS license.

¹To whom correspondence may be addressed. Email: lewis.lanier@ucsf.edu or mocarski@emory.edu.

This article contains supporting information online at www.pnas.org/lookup/suppl/doi:10.1073/pnas.1904319116/-DCSupplemental.

receptor-interacting protein kinase (RIPK)1 and RIPK3 regulate alternate fate outcomes of either apoptosis or necroptosis (12). A comparable complex can form independently of DR ligation downstream of Toll-like receptor (TLR)3 or TLR4, T cell receptor (TCR), or Z-nucleic acid binding protein (ZBP)1. Autoproteolytic cleavage of oligomerized CASP8 executes CASP3-mediated apoptosis, either directly or following Bid cleavage. Importantly, CASP8 prevents RIPK3-dependent, mixed-lineage kinase domain-like (MLKL)-mediated necroptosis. *Casp8*^{-/-} mice exhibit midgestational developmental failure, a phenotype that is fully reversed by elimination of RIPK3, RIPK3 kinase activity, or MLKL. *Casp8*^{-/-}*Ripk3*^{-/-} (double-knockout, DKO) or *Casp8*^{-/-}*Ripk3*^{K51A/K51A} mice are viable, fertile, and immunocompetent (13–16). CASP8 and FADD have been implicated in cytokine signaling via NF- κ B and MAP kinase pathways (12), as well as during T cell proliferation (17), although these particular observations are likely to result from unleashed RIPK3 activity (15). CASP8-deficient T cells complete thymic development but undergo necroptosis following TCR stimulation in the periphery (18–21), a phenotype that is reversed when combined with RIPK3-deficiency (22–24). Investigations into death-dependent and death-independent functions of CASP8 must avoid postthymic TCR-mediated induction of necroptosis.

MCMV is a natural mouse pathogen where infection drives a robust and lifelong CD8 T cell response that controls acute infection and maintains latency (5). This herpesvirus encodes cell death suppressors targeting CASP8 and RIPK3 (15, 25) to sustain virus replication and dissemination in the host by counteracting antiviral host defense mechanisms (26–28). Despite the first-line contribution of death pathways to cell-autonomous mammalian antiviral host defense, DKO mice mount robust immune cell activation following MCMV infection (13, 29, 30). Indeed, young adult DKO mice exhibit enhanced conventional and inflationary CD8 T cell responses in comparison with *Casp8*^{+/+}*Ripk3*^{-/-} (HET) littermate controls or WT C57BL/6 mice (13, 30), implicating CASP8 in restraining T cell responses. Previous studies have shown that virus-specific CD8 T cell numbers trend higher in *Lck*^{Cre}*Fadd*^{td}*Ripk3*^{-/-} mice infected with mouse hepatitis virus (24) but not in *CD4*^{Cre}*Casp8*^{lox/lox}*Ripk3*^{-/-} mice infected with lymphocytic choriomeningitis virus (LCMV) (22). These observations prompted our investigation of CASP8 function in regulating virus-specific T cell responses in mice with combined deficiency in CASP8 and RIPK3. Notably, dendritic cell (DC) numbers are elevated compared with control mice during the acute phase of MCMV infection in DKO mice (30), raising a question of whether CD8 T cell hyperaccumulation in these mice results from T cell-autonomous dysregulation or environmental changes due to the absence of CASP8.

In the present study, we show that DKO CD8 T cells hyperaccumulate independently of the environmental milieu of DKO mice following MCMV infection, attributable to an increase in proliferation rather than a deficit in cell death. These mutant mice exhibit an initial enhancement of conventional and inflationary epitope-specific CD8 T cells due to the hyperaccumulation of KLRG1^{hi}CD127^{lo} terminal effector subsets. Paradoxically, even though the inflationary T cell subset is enhanced over the initial few weeks of infection, the response is not sustained long-term. Our data reveal a death-independent role of CASP8 in restricting CD8 T cell proliferation during the expansion phase following virus infection and in establishing a set point for memory inflation during herpesvirus infection.

Results

Antiviral CD8 T Cells in DKO Mice Hyperaccumulate Early During Viral Infection. The MCMV-specific CD8 T cell immune response remains robust despite combined deficiency in CASP8 and RIPK3 (30). CASP8-specific contribution to CD8 T cell response kinetics in MCMV K181-BAC-infected WT, HET, and DKO mice

was assessed on days 5, 7, 9, and 14 postinfection (pi). Although splenic CD8 T cell numbers were comparable on day 5 (Fig. 1A), DKO mice showed sharply higher peak numbers on day 7 pi than controls but then contracted to a level that was indistinguishable in all 3 genotypes by 14 d pi (dpi). Splenic CD4 T cell numbers expanded and contracted similarly in the 3 mouse genotypes (Fig. 1B). This pattern reinforces a role for CASP8 in restricting CD8 T cell expansion (30) without contributing to contraction, providing clarity to an area that has been extensively studied (8).

To investigate MCMV-specific CD8 T cell kinetics, we used epitope-specific major histocompatibility complex (MHC) class I tetramers to follow the conventional M45-specific CD8 T cell response that dominates early after MCMV infection, as well as to assess the inflationary M38- and IE3-specific responses that are first detected early and continue to rise during long-term infection (6, 31). All epitope-specific subsets accumulated to significantly higher numbers and percentages in DKO mice compared with WT or HET controls (Fig. 1C–E), suggesting an overall enhanced antiviral CD8 T cell response in mice lacking CASP8 and RIPK3. Both numbers (Fig. 1C, Upper) and percentages (Fig. 1C, Lower) of M45-specific CD8 T cells rose more dramatically between 5 and 7 dpi in DKO than in control mice and then contracted over the subsequent week. M38 and IE3 epitope-specific CD8 T cell numbers also showed more dramatic expansion over this time (Fig. 1D and E). Numbers of M38 and IE3 epitope-specific CD8 T cells decreased through days 9 and 14 pi, although IE3-specific T cells exhibited ever higher proportions in DKO mice, consistent with an inflationary pattern (6, 31). These data reinforce the role of CASP8 in restraining the expansion of both conventional and inflationary epitope-specific CD8 T cells early during MCMV infection (30).

Effector CD8 T cells exhibit heterogeneity in expression of KLRG1 and CD127, surface markers that define distinct subsets (2, 3). When the characteristics of accumulating virus-specific CD8 T cells were evaluated at 7 dpi in DKO mice, KLRG1^{hi} cells predominated within the M45-specific subset, particularly within the KLRG1^{hi}CD127^{lo} terminally differentiated effector population (Fig. 1F). In contrast, less terminally differentiated KLRG1^{lo} subsets (KLRG1^{lo}CD127^{hi} and KLRG1^{lo}CD127^{lo}) expanded and contracted very modestly in all 3 genotypes. Following this peak response, T cell subsets contracted regardless of genotype. Consistent with differences in cell numbers, the percentage of M45-specific KLRG1^{hi}CD127^{lo} CD8 T cells predominated at 7 dpi in DKO (Fig. 1G) compared with control mice. Similar enhancement of KLRG1^{hi} subsets was observed with inflationary epitopes M38 (SI Appendix, Fig. S1A and B) and IE3 (SI Appendix, Fig. S1C and D) at this early time. Although this enhancement was not related to differential IL-2 production by DKO CD4 T cells (SI Appendix, Fig. S1E), CD8 T cell-dependent IL-2 production may have contributed (32). Thus, the higher peak CD8 T cell levels in DKO mice is mostly due to accumulating KLRG1^{hi} effector cells. Taken together, these data show that CASP8 naturally restrains the accumulation of KLRG1^{hi} subsets in response to MCMV infection, with a dramatic impact on more terminally differentiated KLRG1^{hi}CD127^{lo} CD8 T cells.

To investigate CASP8-dependent antiviral CD8 T cell hyperaccumulation in another CASP8-deficient genetic background, we compared *Casp8*^{-/-}*Ripk3*^{K51A/K51A} mice (16) to *Ripk3*^{K51A/K51A}, *Ripk3*^{-/-}, and DKO mice. The *Ripk3*^{K51A/K51A} allele lacks proinflammatory kinase activity but retains RIPK3 RIP homotypic interaction motif (RHIM) interactions (16). At 7 dpi, DKO and *Casp8*^{-/-}*Ripk3*^{K51A/K51A} mice showed parallel increases in both numbers and proportions of M45-specific CD8 T cells above those in control *Ripk3*^{-/-}, *Ripk3*^{K51A/K51A}, and WT mice (Fig. 1H and I), consistent with CASP8 restraint on expansion.

To assess the influence of CASP8 on the CD8 T cell response to another herpesvirus, *Casp8*^{-/-}*Ripk3*^{K51A/K51A} mice were infected

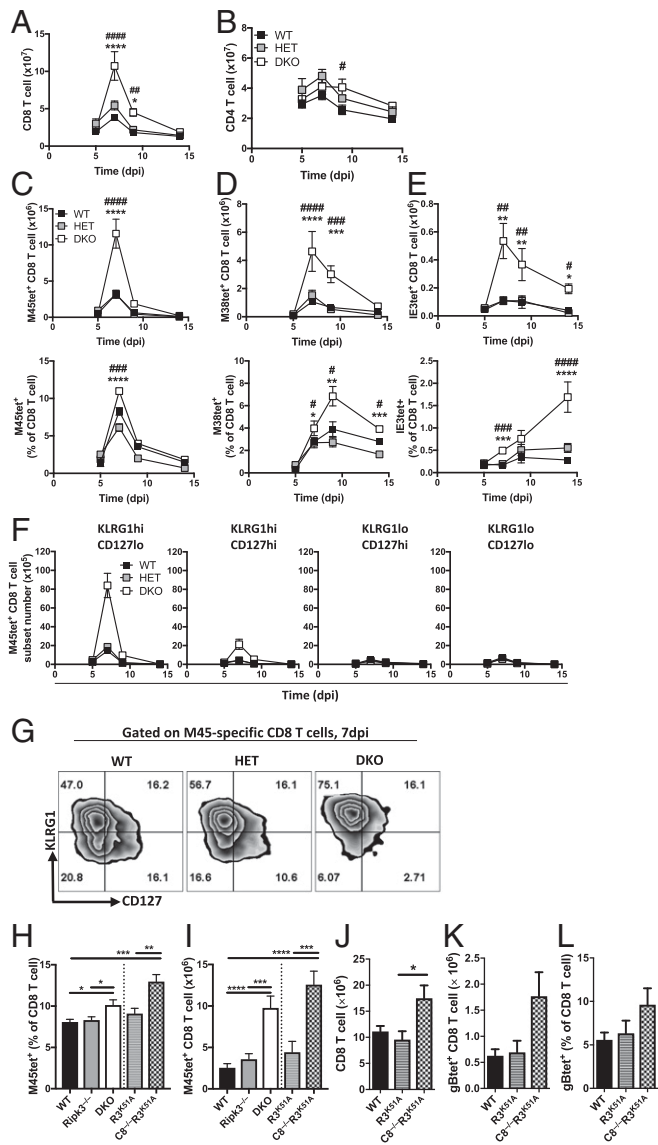


Fig. 1. Impact of CASP8 on T cell responses early during MCMV infection. (A–G) Splenic T cell response in 6- to 8-wk-old WT, HET, and DKO mice inoculated intraperitoneally with 1×10^6 PFU/mouse of MCMV strain K181-BAC and evaluated on days 5, 7, 9, and 14 pi. Splenocytes were subjected to flow cytometry using tetramers and antibodies specific for the indicated cell-surface markers. Graphs comparing total mean numbers of CD8 (A) and CD4 (B) T cells, levels of M45 (M45tet⁺, C), M38 (M38tet⁺, D), or IE3 (IE3tet⁺, E) tetramer-positive CD8 T cells, depicted as mean numbers (Upper) and frequencies (Lower), effector subsets of M45tet⁺ CD8 T cells (F), and representative zebra plots with the percentages of indicated subsets of M45tet⁺ CD8 T cells at 7 dpi (G). All data (with the exception of zebra plots) are shown as mean \pm SEM and represent at least 2 independent experiments using $n = 5$ mice per group. Significant differences between DKO and WT (*) or between DKO and HET (#) mice are indicated as * or # $P < 0.05$; ** or ## $P < 0.01$; *** or ### $P < 0.001$; **** or #### $P < 0.0001$. (H–L) T cell response patterns in 6- to 8-wk-old WT, *Ripk3*^{-/-}, *Ripk3*^{K51A/K51A} (*R3*^{K51A}), DKO, and *Casp8*^{-/-}*Ripk3*^{K51A/K51A} (*C8*^{-/-}*R3*^{K51A}) mice at 7 dpi, infected and evaluated as described in A. Bar graphs showing percentages (H) and numbers (I) of M45tet⁺ CD8 T cells. All data are presented as mean \pm SEM and represent 2 independent experiments using $n = 5$ mice per group. (J–L) T cell response patterns in spleens from WT, *R3*^{K51A}, and *C8*^{-/-}*R3*^{K51A} mice inoculated via the footpad route with 2×10^6 PFU per mouse of HSV-1 (KOS strain) and evaluated at 7 dpi. Bar graphs showing total CD8 T cell numbers (J), as well as numbers (K) and percentages (L) of gB tetramer-specific CD8 T cells (gBtet⁺). All data are presented as mean \pm SEM and represent 1 experiment with $n = 5$ mice per group. * $P < 0.05$; ** $P < 0.01$; *** $P < 0.001$; **** $P < 0.0001$.

with herpes simplex virus (HSV)-1. A similar enhanced pattern of total (Fig. 1J) as well as gB-specific CD8 T cells (Fig. 1K and L) was observed in the *Casp8*^{-/-}*Ripk3*^{K51A/K51A} mice compared with *Ripk3*^{K51A/K51A} or WT controls. Thus, CASP8-dependent regulation of virus-specific CD8 T cells occurs after infection with a primate alphaherpesvirus in a pattern similar to a natural rodent betaherpesvirus.

Early CD8 T Cell Inflationary Response in DKO Mice Collapses During Long-Term Infection. The enhanced responses observed in DKO mice early during infection prompted investigation of long-term infection. Following contraction, the percentages (Fig. 2A) and numbers (Fig. 2B) of splenic M45-specific CD8 T cells at 8 and 25 wk pi (wpi) remained low in WT, HET, and DKO mice. KLRG1^{lo}CD127^{hi} Tcm-like cells predominated at 25 wpi (Fig. 2C), indicating that conventional antiviral CD8 T cell memory developed independently of CASP8 function (6). Strikingly, DKO mice did not exhibit CD8 T cell memory inflation at 25 wpi, even though WT and HET control mice exhibited comparable memory inflation in both frequency (Fig. 2D) and number (Fig. 2E) of IE3-specific T cells that show a predominant KLRG1^{hi}CD127^{lo} effector

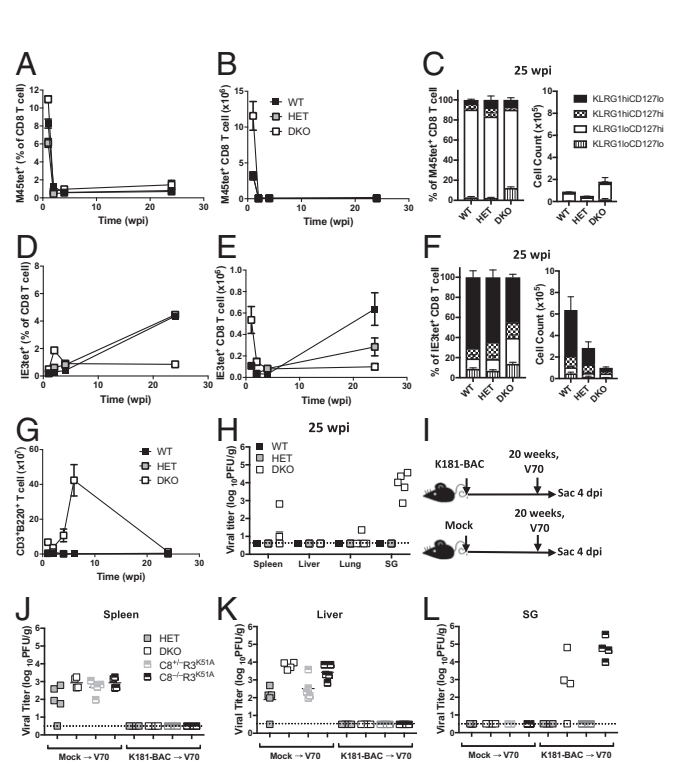


Fig. 2. Impact of CASP8 on T cell response patterns during long-term virus infection. (A–G) Splenic T cell response in WT, HET, and DKO mice infected and evaluated as described in Fig. 1, evaluated through 25 wpi. Graphs showing frequencies and numbers of splenic M45tet⁺ CD8 T cells (A and B) at 1, 2, 4, and 25 wpi, as well as proportions and numbers of KLRG1 and CD127 subsets within M45-specific CD8 T cells at 25 wpi (C), splenic IE3tet⁺ CD8 T cells (D and E) at 1, 2, 4, and 25 wpi, as well as the proportions and numbers of KLRG1 and CD127 subsets within IE3-specific CD8 T cells at 25 wpi (F), and numbers of B220⁺CD3⁺ abnormal splenic T cells through 25 wpi (G). Data are presented as mean \pm SEM (H) Titers of virus in spleen, liver, lungs, and SG at 25 wpi obtained by plaque assay. Panels represent at least 2 independent experiments with $n \geq 4$ per group. (I–L) MCMV V70 strain (1×10^5 PFU by intraperitoneal inoculation route) challenge of WT, DKO, and *C8*^{-/-}*R3*^{K51A} mice infected with K181-BAC (or mock) 20 wk previously, showing experimental plan (I), as well as virus titers in spleen (J), liver (K), and SG (L) at 4 d postchallenge. Dash line in H–L indicates the limit of detection of the plaque assay. Data were collected from 1 experiment with $n \geq 5$ per group.

T cell phenotype (Fig. 2F). In WT mice, memory inflation depends on continuous replenishment by new effector cells that differentiate from naïve or Tcm pools in response to sporadically expressed viral antigens (5, 6). The lack of IE3-specific memory inflation in DKO mice was accompanied by lower numbers of all cell subsets, especially KLRG1^{hi}CD127^{lo} effector T cells (Fig. 2F), which had collapsed by 25 wpi despite the earlier accumulation of KLRG1^{hi} cells (SI Appendix, Fig. S1 C and D). This pattern suggested a failure in the expected (5, 6) recruitment and maintenance of newly activated effector T cells over the long-term in DKO mice. The patterns of M45-, IE3-, and M38-specific memory CD8 T cells in blood of DKO and *Casp8*^{-/-}*Ripk3*^{K51A/K51A} mice (SI Appendix, Fig. S2 A–C) were comparable to splenic patterns, indicating that CASP8-deficient mice exhibited global rather than organ-specific compromise. This phenotype shows that CASP8 functions as a determinant of memory inflation.

Abnormal B220⁺CD3⁺ T cells accumulate in aging DKO mice (13, 14, 29, 30), a phenomenon that has been ascribed to CASP8 function downstream of FADD signaling (11, 33). Given that abnormal T cells have the potential to occupy space in lymphoid organs and prevent accumulation of inflationary T cells, we sought to investigate the consequences of long-term MCMV infection on splenic B220⁺CD3⁺ T cell levels. Even though DKO mice exhibited accumulation of these abnormal T cells through 8 wpi, numbers decreased dramatically (40-fold) by 25 wpi, from 400 million cells per spleen to less than 10 million cells per spleen (Fig. 2G). Thus, accumulation of abnormal T cells in DKO mice was actually dampened by long-term MCMV infection. This reduction in B220⁺CD3⁺ T cell accumulation occurred in the same time frame as the collapse of virus-specific memory inflation, although any relationship between the two will require further investigation.

Given evidence that sporadic reactivation sustains memory inflation via direct antigen presentation to CD8 T cells (6, 7), we next evaluated viral persistence. Somewhat to our surprise given the robust T cell immune response, persistent MCMV replication was detected in the salivary glands (SG) of DKO mice at 25 wpi (Fig. 2H). Virus was also detected sporadically in other organs in a pattern that was distinct from control mice where virus replication was held in check (5). CD4 T cells provide crucial immune control of MCMV within SGs (34, 35), a key site of viral persistence even in WT mice (5). Interestingly, this persistence occurred in DKO mice despite enhanced levels of IFN- γ ⁺ CD4 T cells detected in spleen and peripheral blood (SI Appendix, Fig. S2 D and E). Our data suggest that the higher viral titers in DKO mice were not attributable to a CD4 T cell defect.

CD8 T cells, particularly the inflationary subsets, have been implicated in protection from reinfection or viral reactivation (36–38). We sought to determine whether infected DKO mice were protected from a secondary challenge. DKO mice displayed a collapse in inflationary CD8 T cell subsets by 16 wpi (SI Appendix, Fig. S2C). At 20 wpi with K181-BAC (or mock-treated) mice were challenged with V70, a virulent strain of MCMV (Fig. 2J) (39). Mice were protected from secondary challenge, as evidenced by the absence of virus in spleen (Fig. 2K) and liver (Fig. 2L) at 4 dpi, when robust V70 virus titers were detected in mice undergoing primary infection. Challenged *Casp8*^{-/-}*Ripk3*^{K51A/K51A} mice showed patterns that were indistinguishable from DKO mice as well as from *Casp8*^{+/-}*Ripk3*^{K51A/K51A} littermate controls. Secondary infection had no apparent impact on persistent virus levels in SGs (Fig. 2L). Thus, despite persistent infection of SGs and a compromised inflationary response, DKO mice develop immunological memory sufficient to combat a secondary challenge with a more virulent strain of MCMV.

Enhanced CD8 T Cell Accumulation Occurs Independently of Viral Replication Levels. Next, we sought to address the mechanism responsible for DKO CD8 T cell hyperaccumulation during the

acute phase of virus infection. Viral antigen load is one critical determinant dictating the magnitude of the antiviral CD8 T cell response (3, 40). To reduce antigen load, mice were treated daily with 5 mg/kg of cidofovir (CDV) starting 3 d before MCMV infection through day 7 (Fig. 3A). This antiviral drug regimen is effective against MCMV without causing side effects (31, 41, 42). Control PBS-treated mice showed splenic titers that were comparable in all mouse genotypes at 3 dpi (43), but titers became more variable as infection was brought under control (Fig. 3B, Left). Following CDV treatment, virus replication was suppressed to below detectable levels in spleen (Fig. 3B, Right) independently of mouse genotype. Nevertheless, the enhanced total (Fig. 3C) and M45-specific (Fig. 3D and E) CD8 T cell responses were sustained in DKO mice compared with WT and HET controls. Taken together, the antiviral CD8 T cell hyperaccumulation in DKO mice appears to occur independently of viral antigen load.

Enhanced Proliferation of CD8 T Cells in DKO Mice. Enhanced accumulation of DKO CD8 T cells occurred between 5 and 7 dpi, a period of clonal T cell expansion that may be influenced by CASP8 function (12, 22, 23). When proliferation of these cells was assessed using flow cytometry (44), the percentage of Ki67⁺ (Fig. 4A) CD8 T cells in DKO mice appeared normal on days 0 and 3, but increased to significantly higher levels than WT between 5 and 7 dpi. To determine whether enhanced proliferation of DKO T cells during the expansion phase was due to reduced apoptosis, cell death was first assessed using fixable viability staining (FVS), a cell-impermeable dye that stains late-stage dead cells regardless of death pathway involved. Upon MCMV infection, there was a similar increase in frequencies of FVS⁺ events by 5 dpi in WT and DKO spleens (Fig. 4B). While the frequencies decreased by 7 dpi in WT mice, levels were sustained in DKO mice. Thus, combined deficiency in CASP8 and RIPK3 does not confer a general survival benefit upon splenocytes responding to virus infection. CASP8-initiated apoptosis is executed by CASP3 (12), a caspase that is normally activated in proliferating T cells (17). When the fluorescently labeled inhibitor of caspases (FLICA) was used to detect CASP3

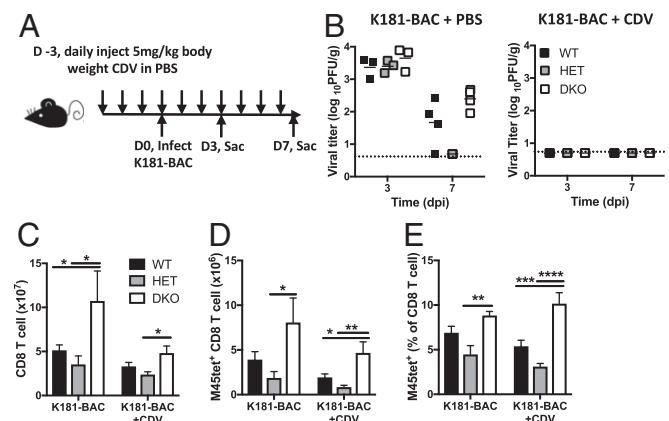


Fig. 3. Pattern of antiviral CD8 T cell response when antigen levels are compromised. Mice were injected daily with 5 mg/kg CDV in PBS (or mock treated) via intraperitoneal inoculation, starting from 3 d before infection (A) with K181-BAC and then killing (Sac) at either 3 or 7 dpi to determine virus levels by plaque assay (B) and T cell response parameters by flow cytometry (C–E). Dash line showing the limits of the detection for the plaque assay. Bar graphs showing numbers of total CD8 T cells (C), as well as numbers (D) and percentages (E) of M45 tetramer-positive CD8 T cells at 7 dpi. Data are presented as mean \pm SEM and represent 2 independent experiments with $n = 4$ mice per group. Significant differences are indicated as * $P < 0.05$; ** $P < 0.01$; *** $P < 0.001$; **** $P < 0.0001$.

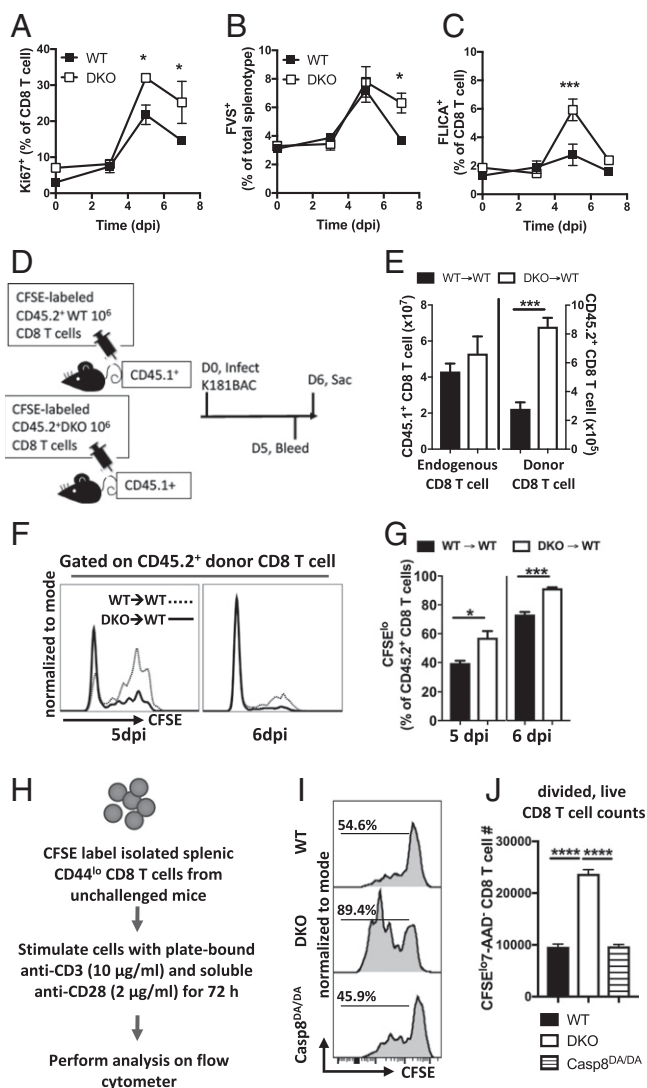


Fig. 4. Assessment of CD8 T cell proliferation and death. (A–C) Analysis of splenocyte proliferation and death during the expansion phase in K181-BAC-infected WT and DKO mice at 0, 3, 5, and 7 dpi. Graphs showing mean percentages \pm SEM of Ki67⁺ CD8 T cells (A), mean frequencies \pm SEM of FVS⁺ dead cells in spleens of WT and DKO mice (B), and mean percentages \pm SEM of FLICA⁺ CD8 T cells, excluding FVS⁺ dead cells (C). (D–G) Proliferation analysis following adoptive transfer. (D) CFSE-labeled CD45.2⁺ splenocytes from WT or DKO mice containing 1×10^6 total CD8 T cells were transferred into CD45.1⁺ WT recipients by intravenous inoculation, followed by intraperitoneal inoculation of MCMV K181-BAC the following day. (E) Bar graphs showing the numbers of CD45.1⁺ endogenous CD8 T cells and CD45.2⁺ donor CD8 T cells at 6 dpi. (F) Representative histograms showing the CFSE distribution of transferred CD8 T cells and (G) bar graphs showing the proportions of the CFSE^{lo} cells of total CD45.2⁺ donor CD8 T cells on days 5 and 6 pi. Data are present as mean numbers \pm SEM and represent 2 independent experiments with $n = 4$ mice per group. (H–J) Assessment of proliferation and signaling following TCR stimulation. CFSE dilution analysis of purified splenic CD44^{lo}CD49d^{lo} CD8 T cells after stimulation with anti-CD3 and CD28 for 72 h (H). Representative plots comparing CFSE division of CD8 T cells from indicated genotypes and numbers showing the proportions of divided CD8 T cells (I). Bar graphs showing the mean numbers \pm SEM of CFSE^{lo}7-AAD⁺ cells recovered in culture following stimulation (J). Significant differences are indicated as * $P < 0.05$; ** $P < 0.01$; *** $P < 0.001$; **** $P < 0.0001$.

activation, the percentages of FLICA⁺ CD8 T cells in DKO mice were similar on days 0 and 3, increased to peak levels at 5 dpi that were higher in DKO mice than WT controls, and decreased by

7 dpi independent of genotype (Fig. 4C). This marked increase in active CASP3⁺ CD8 T cells at 5 dpi may have resulted from either: (i) more death of CD8 T cells during the expansion phase, which would likely be a consequence of Bim-dependent intrinsic death (11); or (ii) greater CD8 T cell proliferation (17, 45), a pattern consistent with higher proportions of Ki67⁺ CD8 T cells at this time point (Fig. 4A). Overall, our data favor enhanced proliferation rather than cell death deficiency conferring the T cell hyperaccumulation pattern characteristic of DKO mice.

In addition to the enhanced T cell response, MCMV-infected DKO mice show increased DC and NK cell numbers (30), either of which may influence T cell response magnitude. To determine whether CD8 T cell hyperaccumulation occurs independently of the DKO environment following virus infection, 5- (and 6)-Carboxyfluorescein diacetate succinimidyl ester (CFSE)-labeled total splenocytes containing 1×10^6 CD8 T cells from CD45.2⁺ WT or DKO mice were transferred into CD45.1⁺ WT recipients, followed by MCMV infection 24 h later (Fig. 4D). CFSE dilution was assessed at 5 and 6 dpi. Endogenous CD45.1⁺ WT T cell numbers remained comparable in either setting (Fig. 4E), indicating that the DKO donor splenocytes did not alter the environment in recipients. Even in this WT-like environment, transferred DKO CD8 T cells exhibited enhanced accumulation at 6 dpi compared with transferred WT T cells (Fig. 4E). In addition, there was a significantly higher proportion of CFSE^{lo} DKO CD8 T cells on days 5 and 6 pi (Fig. 4F and G), indicating increased cell division compared with transferred WT cells. Thus, the enhanced proliferation of DKO CD8 T cells following viral infection occurs independently of the DKO environmental milieu.

Increased cell division has been observed with CD8 T cells purified from DKO as well as from *Lck^{Cre}FADD^{dd}Ripk3^{-/-}* mice subjected to TCR stimulation (24, 30), suggesting that T cell-specific disruption of CASP8 or FADD is sufficient to enhance cell proliferation once the potential to unleash necroptosis has been eliminated. It is important to note that a greater proportion of CD8 T cells in these genotypes showed up-regulated CD44 (30), an activated state that may confer greater proliferative potential. To assess proliferation of CD44^{lo} DKO CD8 T cells, purified splenic CD44^{lo} CD8 T cells were labeled with CFSE, stimulated with anti-CD3 and anti-CD28 antibodies for 72 h, and then subjected to flow cytometry analysis (Fig. 4H). More than 99% of these purified CD8 T cells lacked activation markers, including CD44, CD11a, and CD49d based on flow cytometry. Upon TCR stimulation, CD44^{lo} DKO CD8 T cells proliferated more vigorously than WT controls, correlating with a higher proportion of CFSE^{lo} cells (Fig. 4I) as well as numbers of CFSE^{lo}7-AAD⁺ divided, live cells (Fig. 4J) in the culture. These data suggest that the enhanced proliferative capacity of DKO CD8 T cells occurs independently of the activation state before TCR stimulation.

Upon recruitment to the DISC, CASP8 undergoes dimerization and autoprocessing, which unleashes the full activities of the enzyme and results in extrinsic apoptosis (15). CASP8 autoprocessing mutant mice (*Casp8^{DA/DA}*) are viable yet retain the basal protease activity sufficient for suppressing necroptosis. These mice support robust T cell proliferation upon TCR stimulation (14, 46). Recent studies using *Casp8^{DA/DA}* myeloid cells have implicated the scaffolding function of CASP8 in the regulation of NF- κ B signaling (47). *Casp8^{DA/DA}* CD8 T cells exhibited proliferative capacity indistinguishable from WT controls that was significantly lower than CASP8-deficient DKO cells (Fig. 4I and J), suggesting that CASP8 autoprocessing and consequent extrinsic apoptosis are not involved in restricting CD8 T cell proliferation. These data predict that CASP8 scaffolding function and basal protease activity provide the crucial signaling that restricts CD8 T cell proliferation.

Discussion

This study demonstrates a vital death-independent role of CASP8 in suppressing CD8 T cell proliferation during herpesvirus infection. In mice lacking both CASP8 and RIPK3, the more terminally differentiated effector CD8 T cells subsets accumulate to significantly higher levels due to enhanced proliferation. Nondeath functions of CASP8 have long been suggested to support cell proliferation (17); however, the classic observations that CASP8-deficient T cells do not activate NF- κ B and proliferate in response to antigen (18, 19) failed to account for the confounding consequences of RIPK3-mediated necroptosis that converts the TCR into a DR (22). This incisive work showed clearly that T cells lacking both CASP8 and RIPK3 respond robustly to TCR stimulation and, importantly, exhibit a normal capacity for NF- κ B activation. Our observations in mice with germline CASP8 and RIPK3 deficiency (13, 30) or germline CASP8 deficiency combined with kinase inactive RIPK3 (16) has revealed that CASP8 restricts CD8 T cell proliferation following TCR stimulation, a result that aligns with current understanding of death signaling (12) but runs opposite the expectations from CASP8 studies before the adverse consequences of RIPK3 kinase activity and necroptosis are taken into full account (17). This dramatic unleashing of TCR-dependent necroptosis (12) has not been sufficiently integrated into the conceptualization of T cell activation (8) and deserves greater study in the signaling field.

Upon infection, activated-naïve mouse CD8 T cells undergo 10,000- to 100,000-fold clonal expansion while differentiating into effector subsets that show distinct cytotoxic function or memory potential (3). Following the elimination of virus, expanded T cells undergo an equally dramatic contraction, leaving a small percentage of memory precursors to survive and differentiate into memory subsets. Such a response ensures robust control of invading pathogens and lifelong immunity without unnecessary cytotoxicity or inflammation that would result from prolonged activation. Bim-mediated Bax/Bak-dependent intrinsic apoptosis plays a dominant role in the contraction phase of the antiviral CD8 T cell response (11). Extrinsic apoptosis and necroptosis are clearly dispensable for contraction, reinforcing the central importance of intrinsic apoptosis in regulating the overall level of an antiviral CD8 T cell response (8). Extrinsic cell death contributes to infected cell-autonomous host defense; whereas, the signaling components exert only nondeath impacts on immune cells that respond to and control infections (12, 25). Thus, the intrinsic and extrinsic death pathways make completely independent contributions to host defense against virus infection.

As a natural pathogen of mice, MCMV has provided many insights into the CD8 T cell response to latent virus infection (5) and here revealed the important role of CASP8 in limiting CD8 T cell expansion. When first described, the CD8 T cell hyperaccumulation in MCMV-infected DKO mice appeared to result from greater DC activation (30), which seemed consistent with a study showing that DC-specific elimination of CASP8 (*CD11c^{Cre}Casp8^{flox/flox}*) in mice enhanced CD8 T cell responses to LCMV clone 13 infection (48). Although CASP8 in DC may dampen the magnitude of the LCMV-specific T cell response, the adoptive transfer studies we performed with MCMV show that enhanced accumulation of DKO CD8 T cells is sustained in a WT environment, because of more robust proliferation. In line with this observation, purified total (30) or naïve CD44^{lo} DKO CD8 T cells proliferate more vigorously than controls following TCR stimulation in culture. Thus, both in vivo and in vitro assessment demonstrates that CASP8 within DCs is not required for hyperaccumulation of T cells that lack CASP8 and RIPK3, even though enhanced proliferation of these cells remains dependent on antigen presentation.

A ripoptosome-like signaling complex forms in T cells following postthymic TCR-dependent antigen stimulation (12), most likely mediated by a CARMA-MALT1-Bcl10 complex at the plasma membrane in association with the receptor. This signalosome complex triggers robust NF- κ B, MAPK, and NFAT activation that is necessary for postthymic signaling that regulates an adaptive immune response (49). In this setting, FADD interacts with MALT1 through DD interaction to recruit CASP8, cFLIP_L, RIPK1, and RIPK3 and form a DISC-like complex (12). TCR stimulation results in autocleavage activation of CASP8 along with the subsequent activation of NF- κ B and CASP3 (50). Although classic studies pointed to the nondeath role of CASP8 in sustaining T cell activation in humans and mice (18, 19), much of this evidence does not account for the confounding requirement for CASP8 to suppress necroptosis. By utilizing a necroptosis-compromised model, we unveil a suppressive rather than supportive role of CASP8 following TCR activation. CASP8 may regulate T cell proliferation through other components in the DISC such as RIPK1, which is key to necroptosis, survival, and activation (51, 52). Thus, increased proliferation of DKO cells may result from enhanced RIPK1-mediated NF- κ B and MAPK activation that is normally checked by CASP8. Notably, this enhanced proliferation of DKO cells occurred independently of IL-2, an NF- κ B- and MAPK-regulated cytokine that drives T cell proliferation (53). Comparable IL-2 production from CD4 T cells was observed independently of CASP8 early during MCMV infection. It is possible that CASP8-deficiency augments signaling transduction in a manner that leads to enhanced CD8 T cell proliferation yet suffices for affecting IL-2 production. IL-2 appears to decrease the TCR signaling threshold of CD8 but not CD4 T cells (54) and CASP8 deficiency may further reduce this threshold, augmenting CD8 T cell proliferation in a normal IL-2 environment. Importantly, proliferative enhancement does not occur in the CASP8-autoprocessing mutant cells, consistent with a contribution of CASP8 scaffolding function and basal catalytic activity (46, 55). Although the precise spatial and temporal relationships remain to be dissected, our studies reveal a role of CASP8 in restricting CD8 T cell proliferation in addition to its core functions in initiating apoptosis and suppressing necroptosis.

Remarkably, the enhanced response of inflationary epitope-specific CD8 T cells is not sustained in DKO mice during chronic MCMV infection. Multiple factors are important for memory inflation (5). Previous studies have shown that *Cd4^{-/-}* and *Il2ra^{-/-}* mice exhibit impaired inflationary CD8 T cell responses (56). However, in the present study we did not observe any defect of IL-2 production or CD4 T cell levels in DKO mice. Preliminary data from our laboratory suggest reduced expression of IL-2R α subunit (CD25) on DKO CD8 T cells over the course of long-term infection, although this requires further investigation. If a low CD25 expression phenotype characterizes long-term infection, signaling through IL-2R in DKO CD8 T cells may become compromised and cut short memory inflation (32, 57). In addition to CD25, OX40 and 4-1BB, 2 costimulatory signaling TNF superfamily receptors, play important roles during memory inflation. Interestingly, 4-1BB-deficient mice mount an enhanced inflationary response that contracts over time (58), a pattern similar to DKO mice. Although this receptor is not known to recruit CASP8 or FADD (15), CASP8 may influence signal transduction through indirect mechanisms, such as in the expression of costimulatory receptors (e.g., CD25, OX40, or 4-1BB) or capacity for signal transduction downstream of these receptors. Sustained memory inflation requires newly activated T effector cells from both T_{cm} and naïve pools, driven by sporadic viral reactivation (6, 7, 59). The vigorous response of the KLRG1^{hi} population early during MCMV infection may disrupt memory CD8 T cell regulation, such that cells fail to sustain the correct signaling to drive memory inflation. Most likely, persistent

MCMV replication in DKO mice generates an environment different from the sporadic reactivation responsible for memory inflation in WT mice (6, 7, 59). It seems likely that persistent replication observed in the absence of CASP8 function dominates the sporadic low-level antigen presentation associated with memory inflation in WT mice (60). A recent study showed reduced memory inflation in mice with persistent active MCMV replication in nasal mucosa even 4 mo pi (61). The failure of viral control and hypomemory inflation in this study seems similar to observations in long-term infected DKO mice, although the mechanism through which active MCMV persistence dampens memory inflation remains to be investigated. A history of LCMV Armstrong infection suppresses MCMV-specific inflammatory CD8 T cell responses (62), raising an important question of whether persistent LCMV clone 13 infection would have a more dramatic impact.

Taking these data together, it seems that possible mechanisms that impair memory inflation include a T cell-autonomous defect or some environmental dysregulation due to CASP8 deficiency in DKO mice. Adoptive transfer and investigations in mice with T cell-specific mutants will help reveal any T cell-autonomous function of this protease necessary for preserving memory inflation. The contraction of B220⁺CD3⁺ abnormal T cells in infected DKO mice (13, 30) indicates a beneficial impact of this virus in ameliorating autoimmune markers that may be tied to signaling changes similar to those that cut short memory inflation. Overall, our observations show that CASP8 is required for sustained T cell inflation during chronic MCMV infection while homeostatic accumulation of abnormal T cells first described in mice with Fas-signaling defects (63) is curtailed by long-term infection with this virus.

The sustained MCMV replication observed in SGs of DKO mice may reflect a failure of infected cells to die or some other defect in immune clearance. The higher virus titers observed in DKO mice are reminiscent of mice lacking both Fas and TNFR1, where overall immune control appears compromised (64). It is possible that extrinsic cell death pathways contribute directly to elimination of MCMV-infected cells; however, the normal activities of virus-encoded CASP8 and RIPK3 inhibitors suggests that the cell-autonomous cell death pathways are naturally suppressed under normal infection conditions (15, 25). The reason for persistent infection of DKO mice as opposed to effective control in WT mice suggests some crucial death-independent role of CASP8 and RIPK3 in the resolution of infection in the SGs. Control of primary MCMV infection at this site is dependent on IFN- γ -producing CD4 T cells (34, 35), whose recruitment or maintenance may be compromised in the absence of CASP8 and RIPK3, even though DKO CD4 T cells in spleen and blood circulation continue to respond robustly over long-term infection. RIPK3 adaptor function may influence T cell recruitment into nonlymphoid sites of infection with another virus (65); however, any impact on CD4 T cell trafficking to SGs remains to be investigated. Altogether, our study shows a surprising role of CASP8 together with RIPK3 in controlling MCMV in SGs but the mechanism remains to be elucidated.

In contrast to CD8 T cells, we observed normal splenic CD4 T cell expansion and contraction in response to K181-BAC strain MCMV infection in DKO mice (Fig. 1B). This phenotype contrasts observations with the V70 strain, where total and cytokine-producing CD4 T cells in DKO mice remained higher through 14 dpi (30). Virulence differences between strains or tissue-culture propagated versus SG-propagated MCMV stocks may contribute to differences in this response. Higher antigen load and augmented infection-induced inflammation during V70 infection may drive the increase of CD4 T cells observed in DKO mice.

Our present study focused on the use of WT, RIPK3-deficient, and RIPK3 kinase inactive mice as controls to unveil the

consequences of CASP8-deficiency without a risk of unleashed necroptosis. RIPK3 kinase activity is necessary for MLKL-executed necroptosis (12) when either CASP8 or FADD is compromised (22, 24). Neither RIPK3-deficiency nor an inactive kinase reduces T cell activation, expansion, or contraction following MCMV or HSV-1 infection. Given the comparable behavior of WT, RIPK3-deficient, and RIPK3-kinase inactive mice, we conclude that the major determinant of T cell hyperaccumulation observed in DKO or *Casp8*^{-/-}*Ripk3*^{K51A/K51A} mice is CASP8. Certainly, future studies utilizing tissue-specific CASP8-deficient mice will address how CASP8 restricts T cell proliferation and the manner in which RIPK3 contributes to this phenotype.

We show an unexpected role of CASP8, a crucial regulator of extrinsic cell death, in dampening CD8 T cell proliferation following TCR stimulation. Furthermore, we show the influence of CASP8 deficiency on persistent virus replication, memory inflation, and autoimmune markers. These are all critical areas to consider for CMV-based immunoprophylaxis and vaccine development as well as in the long-term consequences of infection with this type of virus.

Materials and Methods

Mice. DKO (13) and *Casp8*^{-/-}*Ripk3*^{K51A/K51A} (16) mice were derived as described previously and back-crossed to >98% on the C57BL/6 background, based on single nucleotide polymorphism scanning analysis (Jackson Laboratories). DKO and HET littermates were generated by mating DKO sires and HET dams and maintained in-house. *Casp8*^{+/-}*Ripk3*^{K51A/K51A} and *Casp8*^{-/-}*Ripk3*^{K51A/K51A} were generated by mating *Casp8*^{+/-}*Ripk3*^{K51A/K51A} parents. Both *Ripk3*^{K51A/K51A} (16) and *Casp8*^{DA/DA} (66) mice were generated on C57BL/6 background mice. C57BL/6 WT and B6.SJL-Ptprca Pepcb/BoyJ (CD45.1) mice were purchased from Jackson Laboratories and bred at Emory University Division of Animal Resources. Age-matched mixed groups of female and male mice were utilized in experiments. Mouse experimental procedures and infections were conducted in accordance with the National Institutes of Health and Emory University Institutional Animal Care and Use Committee guidelines.

Flow Cytometry, Cell Death Assays, In Vitro CD8 T Cell Proliferation, and Statistical Analysis. Spleens were harvested and processed to splenocytes that were stained with indicated antibodies as described in *SI Appendix, Materials and Methods*. Actively proliferating cells were detected by staining intracellular Ki67. For death assessment, splenocytes were stained with FVS to identify late-stage (permeable) dead cells. FLICA or annexin V⁺ cells were assessed following FVS⁺ dead cells exclusion. Data were acquired by flow cytometry (BD LSRII cytometer and FACSDiva Software; BD Biosciences), analyzed with FlowJo (TreeStar), and graphed with Prism 7 (GraphPad). Statistical analyses were performed by unpaired 1-way or 2-way ANOVA with Tukey analysis using GraphPad Prism 7, where $P \leq 0.05$ was considered significant.

For in vitro CD8 T cell proliferation assessment, purified B220⁺CD3⁺CD4⁻CD44^{lo} CD8 T cells were stimulated with plate-bound anti-CD3 (10 μ g/mL) and soluble anti-CD28 (2 μ g/mL) for 72 h at 37 °C, and then stained with Abs for analysis by flow cytometer, as described in *SI Appendix, Materials and Methods*.

CD8 T Cell Adoptive Transfer. Total CD45.2⁺ splenocytes from naïve WT or DKO mice were labeled with 0.5 μ M CFSE (Invitrogen) in PBS for 10 min at 37 °C. CD45.2⁺ splenocytes that contained 1×10^6 CD8 T cells were transferred intravenously into CD45.1⁺ WT mice, followed by MCMV infection of recipient mice at 1 d posttransfer.

ACKNOWLEDGMENTS. We thank Sam Speck (Emory University) and Rafi Ahmed (Emory University) for reagents and discussion; Joseph Sun (Memorial Sloan Kettering Institute) and Colleen Lau (Memorial Sloan Kettering Institute) for insightful discussion; the National Institute of Health Tetramer Core Facility for MHC class I tetramers; and the Emory Vaccine Center Flow Core for materials and operating assistance. This project was supported by Public Health Service Grants R01 AI020211 and AI118853 (to E.S.M.) and AI068129 (to L.L.L.).

1. I. A. Parish, S. M. Kaech, Diversity in CD8(+) T cell differentiation. *Curr. Opin. Immunol.* **21**, 291–297 (2009).
2. S. M. Kaech, W. Cui, Transcriptional control of effector and memory CD8+ T cell differentiation. *Nat. Rev. Immunol.* **12**, 749–761 (2012).
3. S. Kurtulus, P. Tripathi, D. A. Hildeman, Protecting and rescuing the effectors: Roles of differentiation and survival in the control of memory T cell development. *Front. Immunol.* **3**, 404 (2013).
4. D. Herndler-Brandstetter *et al.*, KLRG1⁺ effector CD8⁺ T cells lose KLRG1, differentiate into all memory T cell lineages, and convey enhanced protective immunity. *Immunity* **48**, 716–729.e8 (2018).
5. P. Klenerman, A. Oxenius, T cell responses to cytomegalovirus. *Nat. Rev. Immunol.* **16**, 367–377 (2016).
6. C. M. Snyder *et al.*, Memory inflation during chronic viral infection is maintained by continuous production of short-lived, functional T cells. *Immunity* **29**, 650–659 (2008).
7. N. Torti, S. M. Walton, T. Brocker, T. Rüllicke, A. Oxenius, Non-hematopoietic cells in lymph nodes drive memory CD8 T cell inflation during murine cytomegalovirus infection. *PLoS Pathog.* **7**, e1002313 (2011).
8. K. P. Li *et al.*, Dying to protect: Cell death and the control of T-cell homeostasis. *Immunol. Rev.* **277**, 21–43 (2017).
9. S. Kurtulus *et al.*, Bim controls IL-15 availability and limits engagement of multiple BH3-only proteins. *Cell Death Differ.* **22**, 174–184 (2015).
10. D. A. Hildeman *et al.*, Activated T cell death in vivo mediated by proapoptotic bcl-2 family member bim. *Immunity* **16**, 759–767 (2002).
11. P. Bouillet, L. A. O'Reilly, CD95, BIM and T cell homeostasis. *Nat. Rev. Immunol.* **9**, 514–519 (2009).
12. B. Tummers, D. R. Green, Caspase-8: Regulating life and death. *Immunol. Rev.* **277**, 76–89 (2017).
13. W. J. Kaiser *et al.*, RIP3 mediates the embryonic lethality of caspase-8-deficient mice. *Nature* **471**, 368–372 (2011).
14. A. Oberst *et al.*, Catalytic activity of the caspase-8-FLIP(L) complex inhibits RIPK3-dependent necrosis. *Nature* **471**, 363–367 (2011).
15. E. S. Mocarski, J. W. Upton, W. J. Kaiser, Viral infection and the evolution of caspase 8-regulated apoptotic and necrotic death pathways. *Nat. Rev. Immunol.* **12**, 79–88 (2011).
16. P. Mandal *et al.*, RIP3 induces apoptosis independent of pronecrotic kinase activity. *Mol. Cell* **56**, 481–495 (2014).
17. S. Shalini, L. Dorstyn, S. Dawar, S. Kumar, Old, new and emerging functions of caspases. *Cell Death Differ.* **22**, 526–539 (2015).
18. N. J. Kennedy, T. Kataoka, J. Tschoop, R. C. Budd, Caspase activation is required for T cell proliferation. *J. Exp. Med.* **190**, 1891–1896 (1999).
19. H. Su *et al.*, Requirement for caspase-8 in NF-kappaB activation by antigen receptor. *Science* **307**, 1465–1468 (2005).
20. K. Newton, A. W. Harris, M. L. Bath, K. G. Smith, A. Strasser, A dominant interfering mutant of FADD/MORT1 enhances deletion of autoreactive thymocytes and inhibits proliferation of mature T lymphocytes. *EMBO J.* **17**, 706–718 (1998).
21. C. M. Walsh *et al.*, A role for FADD in T cell activation and development. *Immunity* **8**, 439–449 (1998).
22. I. L. Ch'en, J. S. Tsau, J. D. Molkentin, M. Komatsu, S. M. Hedrick, Mechanisms of necroptosis in T cells. *J. Exp. Med.* **208**, 633–641 (2011).
23. I. L. Ch'en *et al.*, Antigen-mediated T cell expansion regulated by parallel pathways of death. *Proc. Natl. Acad. Sci. U.S.A.* **105**, 17463–17468 (2008).
24. J. V. Lu *et al.*, Complementary roles of Fas-associated death domain (FADD) and receptor interacting protein kinase-3 (RIPK3) in T-cell homeostasis and antiviral immunity. *Proc. Natl. Acad. Sci. U.S.A.* **108**, 15312–15317 (2011).
25. E. S. Mocarski, W. J. Kaiser, D. Livingston-Rosanoff, J. W. Upton, L. P. Daley-Bauer, True grit: Programmed necrosis in antiviral host defense, inflammation, and immunogenicity. *J. Immunol.* **192**, 2019–2026 (2014).
26. J. W. Upton, W. J. Kaiser, E. S. Mocarski, Virus inhibition of RIP3-dependent necrosis. *Cell Host Microbe* **7**, 302–313 (2010).
27. J. W. Upton, W. J. Kaiser, E. S. Mocarski, DAI/ZBP1/DLM-1 complexes with RIP3 to mediate virus-induced programmed necrosis that is targeted by murine cytomegalovirus vIRA. *Cell Host Microbe* **11**, 290–297 (2012).
28. L. P. Daley-Bauer *et al.*, Mouse cytomegalovirus M36 and M45 death suppressors cooperate to prevent inflammation resulting from antiviral programmed cell death pathways. *Proc. Natl. Acad. Sci. U.S.A.* **114**, E2786–E2795 (2017).
29. W. J. Kaiser *et al.*, RIP1 suppresses innate immune necrotic as well as apoptotic cell death during mammalian parturition. *Proc. Natl. Acad. Sci. U.S.A.* **111**, 7753–7758 (2014).
30. Y. Feng *et al.*, Remarkably robust antiviral immune response despite combined deficiency in caspase-8 and RIPK3. *J. Immunol.* **201**, 2244–2255 (2018).
31. C. M. Snyder, K. S. Cho, E. L. Bonnett, J. E. Allan, A. B. Hill, Sustained CD8+ T cell memory inflation after infection with a single-cycle cytomegalovirus. *PLoS Pathog.* **7**, e1002295 (2011).
32. S. Feau, R. Arens, S. Togher, S. P. Schoenberger, Autocrine IL-2 is required for secondary population expansion of CD8(+) memory T cells. *Nat. Immunol.* **12**, 908–913 (2011).
33. R. Watanabe-Fukunaga, C. I. Brannan, N. G. Copeland, N. A. Jenkins, S. Nagata, Lymphoproliferation disorder in mice explained by defects in Fas antigen that mediates apoptosis. *Nature* **356**, 314–317 (1992).
34. S. Jonjić, W. Mutter, F. Weiland, M. J. Reddehase, U. H. Koszinowski, Site-restricted persistent cytomegalovirus infection after selective long-term depletion of CD4+ T lymphocytes. *J. Exp. Med.* **169**, 1199–1212 (1989).
35. S. M. Walton *et al.*, Absence of cross-presenting cells in the salivary gland and viral immune evasion confine cytomegalovirus immune control to effector CD4 T cells. *PLoS Pathog.* **7**, e1002214 (2011).
36. S. M. Jeitziner, S. M. Walton, N. Torti, A. Oxenius, Adoptive transfer of cytomegalovirus-specific effector CD4+ T cells provides antiviral protection from murine CMV infection. *Eur. J. Immunol.* **43**, 2886–2895 (2013).
37. C. O. Simon *et al.*, CD8 T cells control cytomegalovirus latency by epitope-specific sensing of transcriptional reactivation. *J. Virol.* **80**, 10436–10456 (2006).
38. B. Polić *et al.*, Hierarchical and redundant lymphocyte subset control precludes cytomegalovirus replication during latent infection. *J. Exp. Med.* **188**, 1047–1054 (1998).
39. D. Livingston-Rosanoff *et al.*, Antiviral T cell response triggers cytomegalovirus hepatitis in mice. *J. Virol.* **86**, 12879–12890 (2012).
40. D. M. Andrews, C. E. Andoniou, P. Fleming, M. J. Smyth, M. A. Degli-Esposti, The early kinetics of cytomegalovirus-specific CD8+ T-cell responses are not affected by antigen load or the absence of perforin or gamma interferon. *J. Virol.* **82**, 4931–4937 (2008).
41. J. C. Lenzo, G. R. Shellam, C. M. Lawson, Ganciclovir and cidofovir treatment of cytomegalovirus-induced myocarditis in mice. *Antimicrob. Agents Chemother.* **45**, 1444–1449 (2001).
42. P. Hadaczek *et al.*, Cidofovir: A novel antitumor agent for glioblastoma. *Clin. Cancer Res.* **19**, 6473–6483 (2013).
43. M. Mitrović *et al.*, The NK cell response to mouse cytomegalovirus infection affects the level and kinetics of the early CD8(+) T-cell response. *J. Virol.* **86**, 2165–2175 (2012).
44. T. Scholzen, J. Gerdes, The Ki-67 protein: From the known and the unknown. *J. Cell. Physiol.* **182**, 311–322 (2000).
45. S. McComb, R. Mulligan, S. Sad, Caspase-3 is transiently activated without cell death during early antigen driven expansion of CD8(+) T cells in vivo. *PLoS One* **5**, e15328 (2010).
46. S. Leverrier, G. S. Salvesen, C. M. Walsh, Enzymatically active single chain caspase-8 maintains T-cell survival during clonal expansion. *Cell Death Differ.* **18**, 90–98 (2011).
47. N. H. Philip *et al.*, Activity of uncleaved caspase-8 controls anti-bacterial immune defense and TLR-induced cytokine production independent of cell death. *PLoS Pathog.* **12**, e1005910 (2016).
48. J. S. Tsau, X. Huang, C. Y. Lai, S. M. Hedrick, The effects of dendritic cell hypersensitivity on persistent viral infection. *J. Immunol.* **200**, 1335–1346 (2018).
49. M. Thome, J. E. Charton, C. Pelzer, S. Hailfinger, Antigen receptor signaling to NF-kappaB via CARMA1, BCL10, and MALT1. *Cold Spring Harb. Perspect. Biol.* **2**, a003004 (2010).
50. A. F. Arechiga *et al.*, Cutting edge: FADD is not required for antigen receptor-mediated NF-kappaB activation. *J. Immunol.* **175**, 7800–7804 (2005).
51. G. S. Salvesen, C. M. Walsh, Functions of caspase 8: The identified and the mysterious. *Semin. Immunol.* **26**, 246–252 (2014).
52. Y. Lin, A. Devin, Y. Rodriguez, Z. G. Liu, Cleavage of the death domain kinase RIP by caspase-8 prompts TNF-induced apoptosis. *Genes Dev.* **13**, 2514–2526 (1999).
53. J. M. Marchingo *et al.*, T cell signaling. Antigen affinity, costimulation, and cytokine inputs sum linearly to amplify T cell expansion. *Science* **346**, 1123–1127 (2014).
54. B. B. Au-Yeung *et al.*, IL-2 modulates the TCR signaling threshold for CD8 but not CD4 T cell proliferation on a single-cell level. *J. Immunol.* **198**, 2445–2456 (2017).
55. T. B. Kang *et al.*, Mutation of a self-processing site in caspase-8 compromises its apoptotic but not its nonapoptotic functions in bacterial artificial chromosome-transgenic mice. *J. Immunol.* **181**, 2522–2532 (2008).
56. C. M. Snyder *et al.*, CD4+ T cell help has an epitope-dependent impact on CD8+ T cell memory inflation during murine cytomegalovirus infection. *J. Immunol.* **183**, 3932–3941 (2009).
57. M. F. Bachmann, P. Wolint, S. Walton, K. Schwarz, A. Oxenius, Differential role of IL-2R signaling for CD8+ T cell responses in acute and chronic viral infections. *Eur. J. Immunol.* **37**, 1502–1512 (2007).
58. I. R. Humphreys *et al.*, Biphasic role of 4-1BB in the regulation of mouse cytomegalovirus-specific CD8(+) T cells. *Eur. J. Immunol.* **40**, 2762–2768 (2010).
59. C. J. Smith, H. Turula, C. M. Snyder, Systemic hematogenous maintenance of memory inflation by MCMV infection. *PLoS Pathog.* **10**, e1004233 (2014).
60. G. Picarda, C. A. Benedict, Cytomegalovirus: Shape-shifting the immune system. *J. Immunol.* **200**, 3881–3889 (2018).
61. S. Zhang, S. Caldeira-Dantas, C. J. Smith, C. M. Snyder, Persistent viral replication and the development of T-cell responses after intranasal infection by MCMV. *Med. Microbiol. Immunol.* **10.1007/s00430-019-00589-7** (2019).
62. J. W. Che, K. A. Daniels, L. K. Selin, R. M. Welsh, Heterologous immunity and persistent murine cytomegalovirus infection. *J. Virol.* **91**, e01386-16 (2017).
63. N. Bidère, H. C. Su, M. J. Lenardo, Genetic disorders of programmed cell death in the immune system. *Annu. Rev. Immunol.* **24**, 321–352 (2006).
64. M. Fleck *et al.*, Apoptosis mediated by Fas but not tumor necrosis factor receptor 1 prevents chronic disease in mice infected with murine cytomegalovirus. *J. Clin. Invest.* **102**, 1431–1443 (1998).
65. B. P. Daniels *et al.*, RIPK3 restricts viral pathogenesis via cell death-independent neuroinflammation. *Cell* **169**, 301–313.e11 (2017).
66. P. Mandal *et al.*, Caspase-8 collaborates with caspase-11 to drive tissue damage and execution of endotoxic shock. *Immunity* **49**, 42–55.e6 (2018).